Original article

Med Lasers 2025;14(3):168-174
https://doi.org/10.25289/ML.25.022
pISSN 2287-8300 • eISSN 2288-0224

MEDICAL LASERS
Engineering Basic Research and Clinical Application

Thermal cycling with focused airflow prevents α-keratin denaturation and structural damage in human hair in Korea: an ex vivo study

Tae-Rin Kwon[1]*, Doohyun Han[1]*, Jungwook Kim[1], Hyoung Jun Kim[1], Byung Ho Yoon[1], Dong Wook Moon[1], Jungkwan Lee[1], Kwang Ho Yoo[2]

[1]*Wellness Solution Development Project, Living Solution Business, Home Appliance Solution Company, LG Electronics, Seoul, Republic of Korea*
[2]*Department of Dermatology, Chung-Ang University Gwangmyeong Hospital, Chung-Ang University College of Medicine, Gwangmyeong, Republic of Korea*

Background: Excessive heat from household styling devices denatures α-keratin, damages the cuticle, and degrades overall hair quality. Conventional blow-dryer temperatures often exceed 90°C, surpassing the safety threshold for keratin fibers. To determine whether combining focused airflow with rapid thermal cycling (peak temperatures ≤60°C) attenuates multiscale hair damage compared with continuous-heat drying.

Methods: Human-hair tresses were assigned either to a focused-flow dryer operating in alternating cool/warm cycles or to a continuous-heat mode. Jet characteristics were quantified using planar particle-image velocimetry, and airflow temperatures were recorded using micro-thermocouples. Post-treatment analyses included scanning electron microscopy (cuticular surface roughness, Ra), single-fiber tensile testing, cross-sectional densitometry (fiber compactness), and confocal Raman spectroscopy (α-helix/disulfide bond integrity).

Results: Thermal cycling with focused airflow increased the central-core flow fraction from 37% to 64% and confined hair-surface peaks to 58°C-60°C. Alternating hot-cold drying reduced cuticlar surface roughness by approximately 7.3%, whereas continuous hat air drying increased roughness by 4.9%. Ultimate tensile strength was essentially preserved (−0.4%) under cycling but fell by 9.4% with uninterrupted heat (p = 0.003). Compactness loss was limited to 33% vs. 50%, and the S-S disulfide bond (~510 cm^{-1})/C-H bending vibration band (~720 cm^{-1}) ratio decreased by only 11% (vs. 19% under continuous heat).

Conclusion: Brief cooling intervals, when paired with a confined airflow, effectively prevented α-keratin denaturation and structural collapse. These findings support a clinically relevant approach to preserving hair-fiber integrity during routine hair care and styling.

Key words: Hair; Spectrum analysis; Raman; Tensile strength

Received August 26, 2025, **Accepted** September 4, 2025

Correspondence
Kwang Ho Yoo
E-mail: psyfan9077@naver.com
ORCID: https://orcid.org/0000-0002-0137-6849

*These two authors contributed equally to this work as the first authors.

INTRODUCTION

Human hair is constantly exposed to a wide range of environmental and cosmetic stressors, including ultraviolet radiation, particulate pollution, chemical treatments, mechanical grooming, and increasingly, high-temperature styling [1]. Epidemiological studies have linked frequent use of blow-dryers and flat irons to a higher incidence of shaft breakage, alopecia, and trichorrhexis nodosa in dermatology clinics [2].

Of all these stressors, heat is the most measurable. Below approximately 60°C, the cuticle, the hair's outermost layer, remains largely intact. However, repeated exposures above this threshold can lift, crack, and erode the cuticle in as few as ten drying cycles [3]. The growing desire for smooth, glossy hair has fueled a sharp rise in heat-based styling, with blow-dryers now among the most commonly reported grooming tools in trichology consultations [4]. Epidemiological studies have linked near-daily blow-drying to increased cases of shaft damage and trichorrhexis nodosa, highlighting the clinical relevance of heat-induced hair injury [5].

Thermal damage correlates strongly with temperature. In a controlled dryer study, Lee et al. [1] observed minimal surface fissuring at 47°C, substantial damage at 61°C, and catastrophic cuticle breakdown at 95°C after just 30 cycles [6]. Differential scanning calorimetry shows that α-keratin begins to unfold between 55°C and 65°C, with enthalpy losses doubling once that range is exceeded [2]. Similarly, single-fiber tensile tests report strength reductions of 20% or more above this threshold [7]. For this reason, maintaining hair surface temperatures below ~60°C is widely accepted as the practical safety limit for damage-free drying [8].

However, continuous hot-air drying causes a steady temperature rise because hair's low thermal diffusivity hinders heat dissipation between successive bursts of hot air [9]. As the hair surface temperature approaches 60°C, α-helical domains unravel, disulfide bonds break, and water loss accelerates, ultimately collapsing the cell membrane complex [8]. Clinically, this manifests as dullness, porosity, and breakage [10].

In contrast, rapid hot-cold cycling introduces brief bursts of ambient air that enhance convective cooling and partially rehydrate the cuticle. This practice not only raises the enthalpic barrier to keratin unfolding but also preserves drying efficiency [11,12]. Still, robust data linking temperature modulation, particularly with flow confinement that protects the scalp periphery, to hair health at multiple scales remains scarce.

To address this gap, we paired a flow-focusing nozzle with alternating warm and cool airflow and compared its effects to continuous hot air using matched ex vivo hair tresses. Through a combination of particle image velocimetry (PIV), micro-thermocouple thermography, scanning electron microscopy, single-fiber tensiometry, hair densitometry, and confocal Raman spectroscopy, we investigated whether brief cooling intervals delivered via a confined jet could keep fiber temperatures below the denaturation threshold and reduce structural, mechanical, and molecular damage. These findings could offer new insights for dermatologic guidance and everyday styling practices.

METHODS

Ethics statement: This secondary analysis used data from the National Health and Nutritional Survey provided in anonymous form. Therefore, Institutional Review Board approval was not sought; however, the study adhered to the principles of the Declaration of Helsinki.

Dryer apparatus and airflow characterization

Drying was performed with a handheld prototype equipped with a flow-focusing nozzle engineered to confine the jet footprint (proprietary geometry). Jet kinematics were measured using PIV (532 nm double-pulse laser, relay optics, high-speed camera; diethyl-hexyl-sebacate [DEHS; Sigma-Aldrich] seeding ~2 μm). From the velocity fields, the full-width at half-maximum (FWHM) and central-core flow fractions were extracted at x = 30 and 100 mm to verify jet collimation.

Temperature acquisition

Fifty-three channels were affixed to an acrylic plate at predefined positions (Fig. 1A). With the hair dryer secured, real-time temperatures were recorded for 1 minute using thermocouples connected to a temperature data acquisition system (Graphtec Data Logger, Midi LOGGER GL840, Max. 20 ch; Graphtec Co.). All tests were conducted at 22°C-24°C and 40%-60% relative humidity. The above content is currently under patent application with the Korean Intellectual Property Office.

Drying regimens and handling

Commercial human-hair tresses (Asian, virgin, 15 cm, ~120 ± 5 fibers; Crown Wig Co., Ltd.) were shampooed with a neutral formulation (pH 6.5; 1 ml per gram of hair^{-1}; 30 seconds massage; 60 seconds rinse) and air-dried for

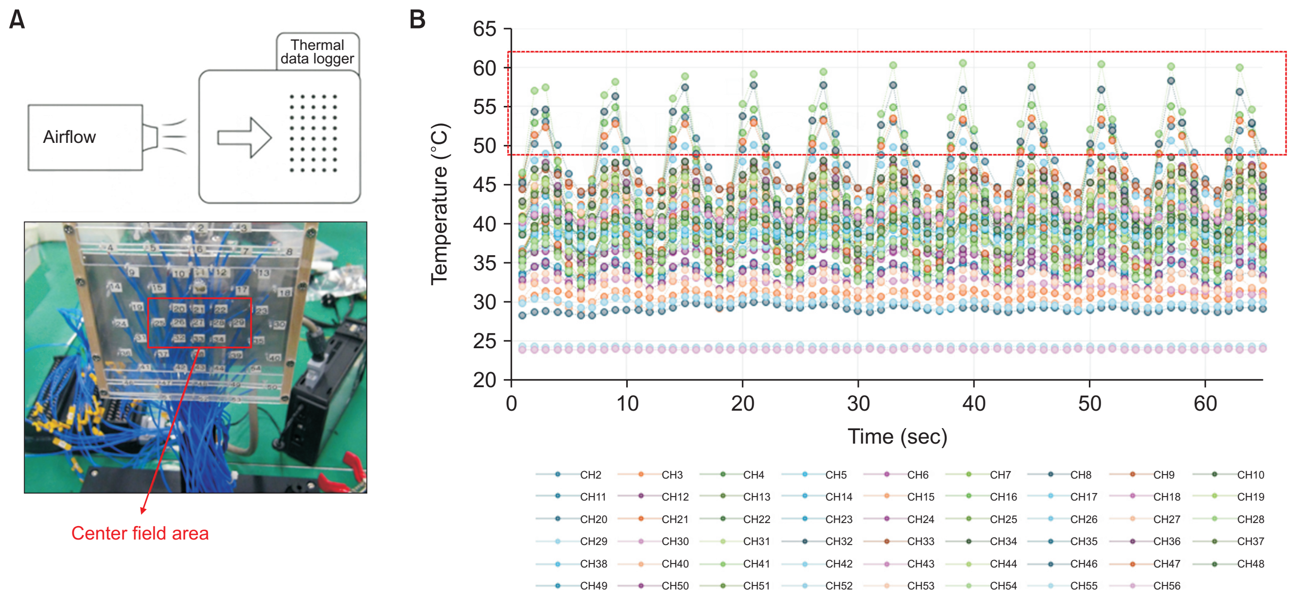

Fig. 1. Temperature profile during alternating hot-cold cycles. (A) Experimental setup showing 53 thermocouples affixed to an acrylic plate for real-time surface air temperature measurement. (B) Representative thermal profile displaying repeated heating (peak ~60°C) and cooling cycles over 10 repetitions during a 1-minute exposure.

24 hours at 22°C-24°C and 40%-60% relative humidity. Two regimens were compared on matched tresses: (1) Alternating hot-cold: warm air (~80°C) alternated with ambient air (~room temperature) for 3 minutes. (2) Continuous hot air: identical volumetric flow at ~80°C without cooling intervals for the same total time. The nozzle-to-tress distance was 10 cm, and tresses were rotated on a motorized jig (30 rpm) for uniform exposure.

Scanning electron microscopy and surface roughness (Ra)

Hair fibers were sputter-coated with Au/Pd (~10 nm) and imaged at 5 kV on a COXEM EM-30 (Mini SEM; COXEM) scanning electron microscope (SEM). Images were analyzed in ImageJ to quantify cuticular surface roughness (Ra; arbitrary units). Briefly, brightness and contrast were automatically adjusted for each image. In total, per group 50 digital SEM images (8-bit) were acquired from five hair segments, and all were then processed using ImageJ software (ImageJ 1.52a; National Institutes of Health).

Single-fiber tensile testing

Ultimate tensile strength was measured with a Unitest M1 (Testone) (gauge length 20 mm; crosshead speed 10 mm/min^{-1}). Individual fibers (n = 50) were tested under each condition, with force reported in gram-force (gf). Where specified, a Tress-MTT175 (Dia-Stron Limited) platform provided gmf-based elastic parameters.

Hair densitometry

Following labeling with dansyl chloride (Dns-Cl), binding and fluorescence increased with the degree of damage, serving as an indirect indicator of increased porosity (i.e., decreased density) [13]. Tresses were Dns-Cl-pretreated and imaged under fixed exposure on an EVOS^{TM} FL Auto2 Imaging System (Thermo Fisher Scientific). Mean pixel intensity within fixed regions of interest was quantified in Image-Pro Plus Program (Media Cybernetics) as a surrogate for optical density; lower intensity indicates reduced cross-sectional compactness.

Raman microspectroscopy

White hair tress bundles (sheep wool; Crown Wig Co., Ltd.) were washed with client-provided shampoo and air-dried. White hair was selected to avoid melanin-related spectral interference in black hair [14,15]. From the washed bundles, >20 individual strands were collected and measured before use. For each dryer mode (test and control), the pre-measured strands were exposed to airflow for 15 minutes; post-use spectra were acquired after cooling. Confocal Raman spectra (Horiba XploRA Plus; Horiba) were baseline-corrected and normalized to a reference band. Assignments included S-S stretching (~510 cm^{-1}), amide I (~1,660 cm^{-1}), and C-H (~720 cm^{-1}). The primary molecular index was the S-S (~510 cm^{-1})/reference (e.g., C-H ~720 cm^{-1}) ratio; lower values indicate greater keratin alteration.

Statistical analysis

The primary endpoint was change in Ra from baseline. Secondary endpoints were peak surface temperature, breaking force (gf), compactness (intensity), and the Raman S-S/reference ratio. Data are presented as mean ± standard deviation. Normality was assessed using the Shapiro–Wilk test and paired two-tailed t-tests (or Wilcoxon) were applied as appropriate. Post-treatment differences were also evaluated via ANCOVA (baseline covariate) and checked in a linear mixed-effects sensitivity model (random effect: stress). Multiplicity was controlled using Holm–Bonferroni; two-sided $p < 0.05$ was considered significant.

RESULTS

Aerodynamic profile of the experimental nozzle

Because peripheral airflow raises scalp temperature without improving drying efficiency, professional dryers favor highly collimated jets. Planar PIV confirmed that the Triple Airfluidics^{TM} system (LG electronics), which is a multilayered airflow architecture that concentrates the core stream and minimizes peripheral energy loss, produces a tightly collimated, core-dominated jet with minimal peripheral turbulence (Fig. 2A, B). The axial velocity profile showed an FWHM of 28.0 mm at x = 70 mm, narrower than typical salon-grade diffusers. Flow-rate mapping at x = 30 and 100 mm demonstrated that >70% of total momentum was confined to the central quadrants, indicating strong directionality. Schlieren visualization confirmed a restricted angular spread (Fig. 2C), supporting targeted drying while limiting peripheral heating. Together, these data indicate that the redesign delivers momentum and heat to the hair surface efficiently while minimizing impact on adjacent areas, which should increase drying rates.

Thermal cycling maintains sub-denaturation peak temperature

Real-time microthermocouple monitoring showed that the alternating hot-cold algorithm generated a consistent sawtooth thermal profile with distinct warm and cool phases (Fig. 1B). Peak fiber temperatures remained within 58°C-60°C, below the α-keratin denaturation threshold (~60°C-65°C), while trough temperatures returned to ~30°C between heating cycles. In contrast, continuous hot-air exposure (data not shown) exceeded 80°C, sustaining a high-risk thermal load. These findings indicate that brief ambient-air bursts effectively cap fiber temperatures below the keratin denaturation range.

Macroscopic hair surface preservation

Surface profilometry showed a significant decline in Ra after thermal cycling (−7.3% ± 2.1%; $p < 0.05$), indicating smoother cuticle surfaces, whereas continuous heat increased Ra (+5.1% ± 1.8%; $p < 0.05$) (Fig. 3A). Cross-sectional compactness showed no change in the cycling group, whereas a significant reduction was observed after continuous heat exposure ($p < 0.05$; Fig. 3B). Raman band intensity ratios (S-S/C-H) declined less with cycling

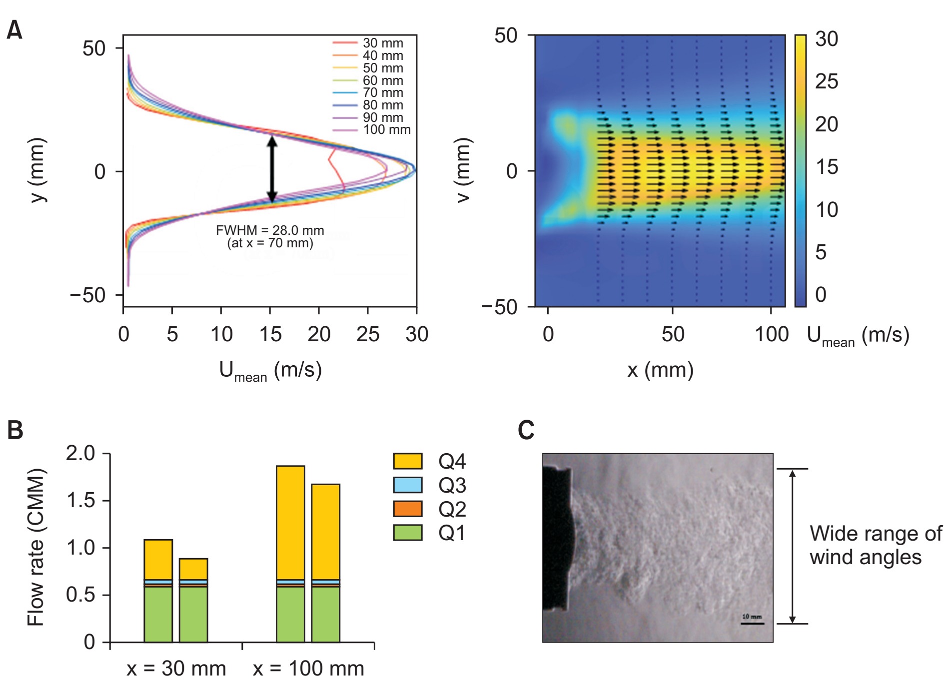

Fig. 2. Airflow characteristics of the tested hair dryer. (A) Cross-sectional velocity distribution and full-width at half-maximum (FWHM) measured 70 mm from the nozzle. (B) Flow rate comparison (cubic meters per minute [CMM]) at x = 30 mm and x = 100 mm, segmented into quartiles: Q1 (innermost jet core), Q2 (near-core annulus), Q3 (peripheral dissipation zone), and Q4 (effective central-core fraction). (C) Schlieren imaging showing angular spread of airflow.

https://doi.org/10.25289/ML.25.022

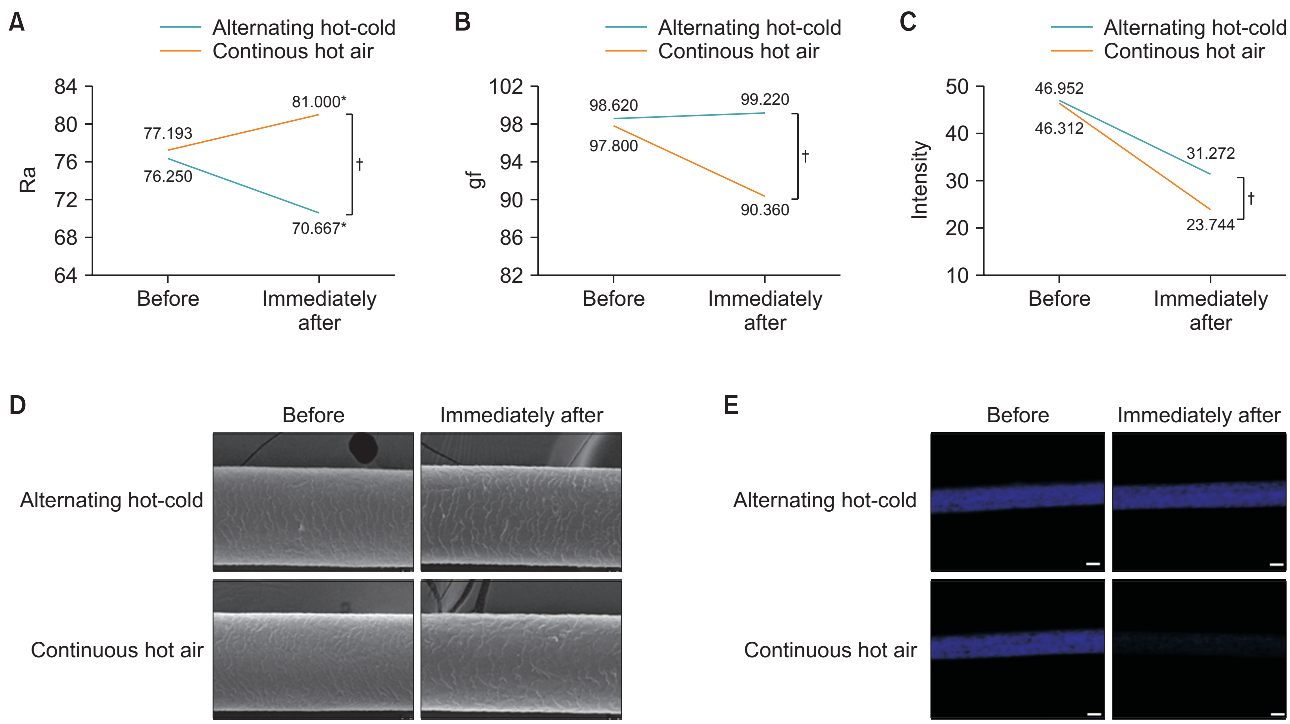

Fig. 3. Hair property changes after drying treatments. (A) Surface roughness (Ra), (B) gram-force (gf), (C) Raman intensity of α-keratin before and after drying with alternating hot-cold versus continuous hot-air mode. (D) Scanning electron microscopy images of cuticle morphology (1,000× magnification; scale bar = 50 µm). (E) Hair density in human hair tress photo image by EVOS^{TM} M5000 Imaging System (scale bar = 200 µm). *$p < 0.05$ by paired t-test, †$p < 0.05$ by repeated-measures ANOVA.

(–14.2%) than with continuous heat (–43.9%) (Fig. 3C), reflecting reduced disulfide disruption. Scanning electron microscopy imaging corroborated these measurements, revealing intact, overlapping cuticle layers after cycling versus lifted and fractured cuticles after continuous heating (Fig. 3D). Cross-sectional densitometry demonstrated a smaller loss of compactness with cycling (33%) than with continuous heat (50%) (Fig. 3E), consistent with reduced dehydration and cortical compaction. Collectively, these results show that hot-cold cycling reduces both cuticular erosion and dehydration-driven contraction.

Molecular-level keratin preservation

Confocal Raman spectroscopy revealed a smaller reduction in mean S-S/C-H ratio after alternating hot-cold airflow (from 19.580 ± 0.621 to 17.346 ± 0.518; $p < 0.05$) than after continuous heat (from 19.064 ± 0.713 to 15.986 ± 0.642; $p < 0.05$) (Fig. 4A). Between-group comparisons confirmed a significant preservation advantage for cycling ($p < 0.05$). Representative spectra showed minimal shifts in amide I (~1,660 cm^{-1}) and S-S (~510 cm^{-1}) peaks with cycling, whereas continuous heating induced pronounced changes (Fig. 4B). Raman heat maps revealed fewer high-damage zones during cycling (Fig. 4C), and high-magnification imaging (Fig. 4D) showed fewer fissures and cortical disruptions. Practically, alternating hot-cold airflow preserves smoothness, hydration, and breakage resistance without prolonging drying time, thus supporting it as a lower-damage alternative to continuous heating.

DISCUSSION

Our data support a unified mechanism in which aerodynamic jet focusing and brief hot-cold pulses jointly constrain thermal dose, thereby blunting the canonical cascade of keratin damage across scales [1]. Planar PIV confirmed that the redesigned nozzle generates a tightly collimated, core-dominated jet with minimal peripheral leakage [16], indicating that momentum and heat are delivered directly to the moisture-bearing hair bundle rather than dissipated into the adjacent scalp or ambient air [2]. Within this spatially confined field, intermittent cooling produced a reproducible sawtooth temperature profile, with peaks remaining below the α-keratin denaturation window (~55°C-65°C) [2]. By contrast, non-cycling controls rapidly exceeded this threshold and maintained sustained exposure within it, a thermal regime known to accelerate secondary-structure transitions and disulfide

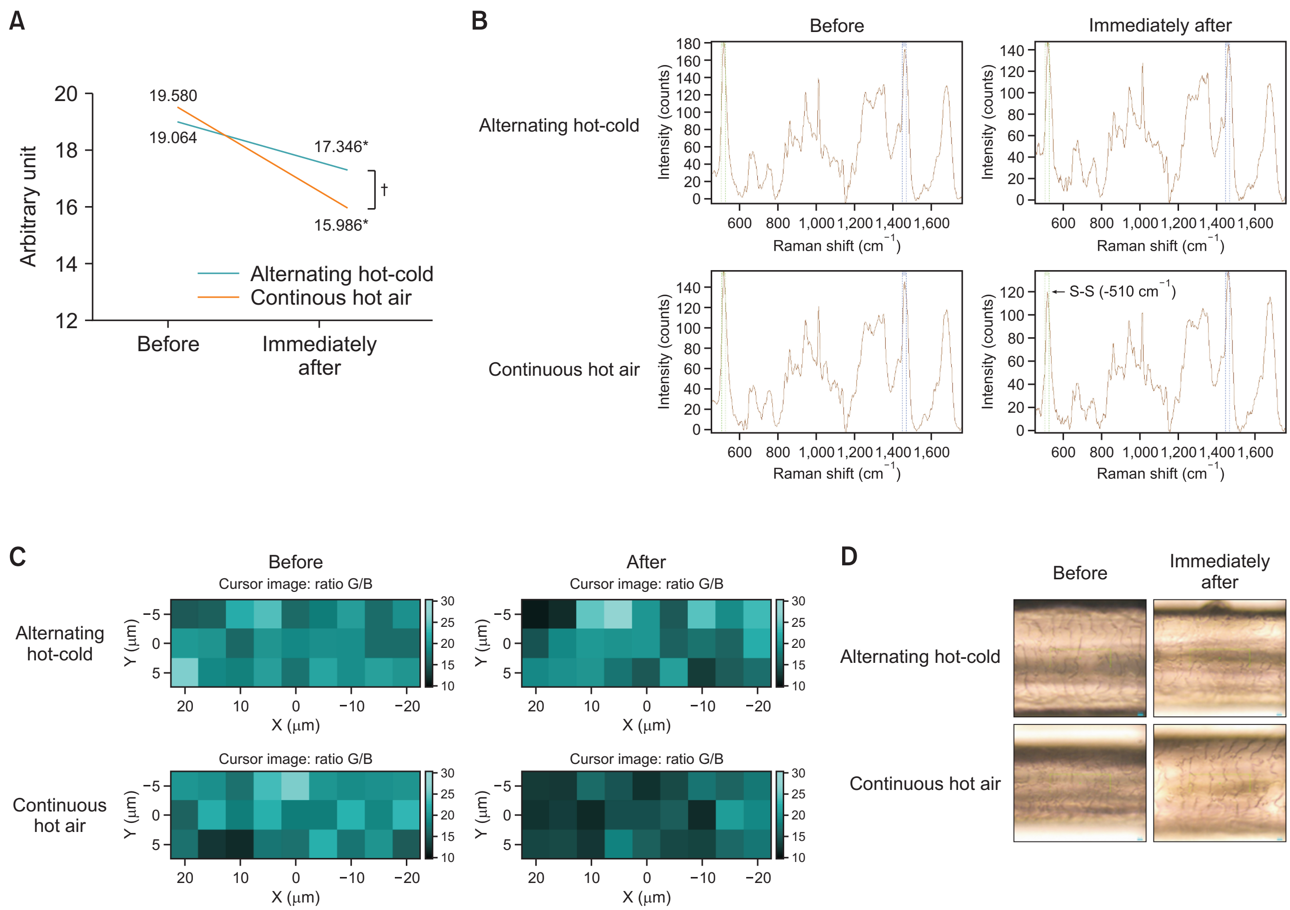

Fig. 4. Raman spectroscopic analysis of hair protein structure. (A) Mean Raman intensity of the α-keratin amide I band before and after treatment. (B) Representative spectra showing greater signal loss following continuous hot air compared to hot-cold cycling. (C) Two-dimensional Raman mapping of protein distribution. (D) Optical microscopy of the hair surface indicates structural degradation following continuous heat exposure (scale bar = 50 μm). *$p < 0.05$ by paired t-test, †$p < 0.05$ by independent t-test.

bond scission [7].

Downstream measurements closely followed this thermal-threshold model. Scanning electron microscopy revealed that cycling preserved smooth, overlapping cuticular plates, while uninterrupted heat led to scale lifting, edge fissuring, and fragmentation. Cross-sectional densitometry showed smaller losses of compactness under cycling [3], suggesting reduced dehydration-driven contraction and better preservation of the cuticle/cell-membrane complex interface [11]. Functionally, single-fiber testing showed preserved breaking force and no increase in stiffness under cycling, whereas continuous heating caused both—a mechanical signature of matrix embrittlement due to accelerated water loss [9]. At the molecular level, Raman band-ratio indices demonstrated less disruption of disulfide bonds and α-helical content with cycling, and spectroscopic "hot spots" were concentrated in continuously heated samples, aligning molecular, mechanical, and morphological evidence.

Taken together, limiting peak temperature in both time (via cooling intervals) and space (via jet confinement) produces multilevel protection, thus preserving cuticle integrity, cortical structure, and protein chemistry without extending drying time [2]. Practically, this low-damage strategy is directly applicable in salon, home, and dermatologic settings, where fiber integrity and patient comfort are critical (e.g., pre-procedure preparation, color longevity) [7].

Key limitations include the ex vivo design, a limited range of phenotypes and cosmetic histories, and a short exposure window. Future work should expand to in situ scalp thermography, longer cumulative exposures, broader hair types, and additional spectroscopic markers to test generalizability. Overall, focused-jet hot-cold pulse drying offers a mechanistically grounded, clinically meaningful approach to preserving hair-fiber integrity by avoiding sustained excursions into the denaturation regime and curbing dehydration-induced embrittlement.

ORCID

Tae-Rin Kwon, https://orcid.org/0000-0002-9892-7714
Doohyun Han, https://orcid.org/0009-0007-1902-5645
Jungwook Kim, https://orcid.org/0000-0003-3639-8391
Hyoung Jun Kim, https://orcid.org/0009-0003-8673-4362
Byung Ho Yoon, https://orcid.org/0000-0001-5779-8357
Dong Wook Moon, https://orcid.org/0000-0001-5564-2893
Jungkwan Lee, https://orcid.org/0000-0002-5365-4740
Kwang Ho Yoo, https://orcid.org/0000-0002-0137-6849

AUTHOR CONTRIBUTIONS

Conceptualization: TRK, KHY. Data curation: TRK, DH, BHY. Formal analysis: TRK, HJK. Investigation: TRK, DH. Methodology: TRK. Project administration: JL. Software: JK, DWM. Validation: KHY. Visualization: JK. Writing–original draft: TRK. Writing–review & editing: all authors.

CONFLICT OF INTEREST

Kwang Ho Yoo is the Editor-in-Chief of the journal but was not involved in the review process of this manuscript. Otherwise, there is no conflict of interest to declare.

FUNDING

None.

DATA AVAILABILITY

Contact the corresponding author for data availability.

ACKNOWLEDGMENTS

None.

SUPPLEMENTARY MATERIALS

None.

REFERENCES

1. Lee Y, Kim YD, Hyun HJ, Pi LQ, Jin X, Lee WS. Hair shaft damage from heat and drying time of hair dryer. Ann Dermatol 2011;23:455-62.
2. Wortmann FJ, Wortmann G, Marsh J, Meinert K. Thermal denaturation and structural changes of α-helical proteins in keratins. J Struct Biol 2012;177:553-60.
3. Essendoubi M, Meunier M, Scandolera A, Gobinet C, Manfait M, Lambert C, et al. Conformation changes in human hair keratin observed using confocal Raman spectroscopy after active ingredient application. Int J Cosmet Sci 2019;41:203-12.
4. Akhtar W, Edwards HG, Farwell DW, Nutbrown M. Fourier-transform Raman spectroscopic study of human hair. Spectrochim Acta A Mol Biomol Spectrosc 1997;53A:1021-31.
5. Barba C, Martí M, Manich AM, Carilla J, Parra JL, Coderch L. Water absorption/desorption of human hair and nails. Thermochim Acta 2010;503-504:33-9.
6. Jamart J, Djaghloul M, Bergheau JM, Zahouani H. Effect of water desorption on the rheology and dynamic response of human hair to a non-contact impact. J Mech Behav Biomed Mater 2015;46:176-83.
7. Kourbaj G, Bielfeldt S, Kruse I, Wilhelm KP. Confocal Raman spectroscopy is suitable to assess hair cleansing-derived skin dryness on human scalp. Skin Res Technol 2022;28:577-81.
8. Yu Y, Yang W, Wang B, Meyers MA. Structure and mechanical behavior of human hair. Mater Sci Eng C Mater Biol Appl 2017;73:152-63.
9. Li C, Du Y, Chen H, Han X, Wu W, Kong X, et al. Transmission infrared micro-spectroscopic study of individual human hair. J Biomed Opt 2023 ;28:116501.
10. Lima CRRDC, Machado LDB, Velasco MVR, Matos JDR. DSC measurements applied to hair studies. J Therm Anal Calorim 2018;132:1429-37.
11. Bories MF, Martini MC, Et MF, Cotte J. Effects of heat treatment on hair structure. Int J Cosmet Sci 1984;6:201-11.
12. Christian P, Winsey N, Whatmough M, Cornwell PA. The effects of water on heat-styling damage. J Cosmet Sci 2011;62:15-27.
13. Sandhu SS, Robbins CR. A sensitive fluorescence technique using dansyl chloride to assess hair damage. J Soc Cosmet Chem 1989;40:287-96.
14. Dos Santos JD, Edwards HGM, de Oliveira LFC. Raman spectroscopy and electronic microscopy structural studies of Caucasian and Afro human hair. Heliyon 2019;5:e01582.
15. Huang Z, Lui H, Chen XK, Alajlan A, McLean DI, Zeng H. Raman spectroscopy of in vivo cutaneous melanin. J Biomed Opt 2004;9:1198-205.
16. Adrian RJ. Particle-imaging techniques for experimental fluid mechanics. Annu Rev Fluid Mech 1991;23:261-304.

How to cite this article: Kwon TR, Han D, Kim J, Kim HJ, Yoon BH, Moon DW, Lee J, Yoo KH. Thermal cycling with focused airflow prevents α-keratin denaturation and structural damage in human hair in Korea: an ex vivo study. Med Lasers 2025;14:168-174. https://doi.org/10.25289/ML.25.022